European Geothermal Congress 2016
Strasbourg, France, 19-24 Sept 2016

Improvements on a Numerical Model of Borehole Heat Exchangers

Anjan Rao Puttige[1], Juan Rodriguez[2], Patricia Monzó[1]*, Fernando Cerdeira[3], Alfredo Fernández[4], Lucia Novelle[4], José Acuña[1], Palne Mogensen[1]

[1]KTH Royal Institute of Technology, Brinellvägen 68, 100 44 Stockholm (Sweden)
[2] EnergyLab, Fonte das Abelleiras s/n, Campus Universidad de Vigo, 36310 Vigo (Spain)
[3]Universidad de Vigo, Maxwell 16, 36310 Vigo (Spain)
[4] Ingeo Investigación Geotérmica, Parque Tecnológico de Galicia, 32901 San Cibrao, Ourense (Spain)
* patricia.monzo@energy.kth.se

Keywords: Monitored installation, borehole heat exchanger, fluid temperature prediction.

ABSTRACT:

In the mathematical simulation of bore fields for ground coupled heat pump (GCHP) systems, it has become a common practice to consider the boreholes as having a uniform temperature. As a rule the boreholes are hydraulically connected in parallel and the small temperature difference between incoming and outgoing heat carrier fluid justifies the assumption that all boreholes have the same uniform temperature in operation. Two simultaneous boundary conditions usually apply: All borehole walls should have a uniform temperature and the heat flow from the bore field should equal the energy needed by the heat pump. This paper describes improvements applied to a previous numerical approach that employs the concept of a highly conductive material (HCM) embedded in the boreholes and connected to a HCM bar above the ground surface to impose a uniform temperature boundary condition at the borehole wall. The original boundary condition with the uniform fluid temperature comes in conflict with the concept of the uniform borehole wall temperature. Between the fluid and the borehole wall there is a thermal borehole resistance. The heat flux increases at the borehole ends and thus also the temperature changes between borehole wall and the fluid. The borehole wall temperature deviates from the uniform assumption and will cause an error in the simulations. This paper presents a correction to that error. Firstly, the improvements to the HCM model are validated for g-function generation, which presents a good agreement with reference solutions. Secondly, the improvements to the HCM model are illustrated to predict fluid temperatures for measured variable daily loads of a monitored GCHP installation. The predicted fluid temperatures are compared with monitored data for about four years. The predicted fluid temperatures deviate from the measured data by less than 1 K during the last monitored year.

1. INTRODUCTION

High efficiency and low environmental impact have made ground coupled heat pump (GCHP) systems an attractive solution for providing space heating and cooling in commercial and residential buildings. An increasing interest in GCHP systems and a steady growth in number of installed units have been seen during the last few years in southern Europe. However, the total installed capacity in southern European countries is still not comparable to the figures in leading countries. The monitored GCHP installation that is subject of study in this paper is situated in the northwest of Spain, a country with relatively less experience in this technology. While a total capacity of about 60 MW is installed in Spain (Arrizabalaga, et al., 2015), in Sweden, recognized as a leading country, the total installed capacity is about 5.6 GW (Gehlin, et al., 2015)

A GCHP system consists of three main components: an indoor circuit in the building, which is connected to the outdoor circuit buried in the ground through the heat pump (except for free cooling operation). The advantage of using the ground as a heat source or sink is derived from the fact that the ground temperature is relatively stable compared to the temperature of the outdoor air.

The outdoor circuit is commonly made up of a closed-loop consisting of a number of vertical U-pipe heat exchangers connected in parallel, called ground heat exchangers (GHE) that comprises the bore field. The outdoor circuit is designed to keep the inlet fluid temperature of the heat pump (outlet fluid temperature of the GHE) within its operational limits and to supply the intended energy demand of the building. To ensure high performance of the heat pump over the years, long term simulation of the thermal response of the GHE is required. Both numerical and analytical methods are utilized to predict the long-term response of the GHE.

When modeling GHE connected in parallel, two simultaneous boundary conditions are usually defined: a

uniform temperature at all boreholes walls and a total heat flow to the bore field, which should be equal to the energy required by the heat pump. The assumption of a uniform borehole wall temperature has its foundation on the parallel hydraulic connection of the boreholes and on the small temperature difference between incoming and outgoing heat carrier fluid.

The numerical approach described in (Monzó et al., 2015) employed the concept of a fictitious highly conductive material (HCM) embedded in the boreholes and connected to a HCM bar above the ground surface to fulfill the two aforementioned boundary conditions. By applying the total bore field flow at the top of the HCM bar, the heat flow is distributed through the HCM to each borehole by satisfying a uniform temperature boundary condition at all the borehole walls. However, the original boundary condition with a uniform fluid temperature comes in conflict with the concept of a uniform temperature at the borehole wall. Because of the thermal resistance between the fluid and the borehole wall and the fact that the heat flux increases at the borehole ends, the temperature at the borehole wall differs from the assumption of a uniform temperature boundary condition at the borehole wall. This paper describes improvements applied to the numerical approach in (Monzó et al., 2015) in order to correct the definition of the boundary condition at the borehole wall. The improved model is validated for the g-function generation. The improved model is also utilized to illustrate daily fluid temperature predictions for variable measured daily loads of a monitored GCHP installation (52 kW) in Baiona (Galicia, Spain). The measured data comprises fluid temperatures and energy flow measurements for about 4 years. The predicted daily fluid temperatures are compared with their corresponding measured fluid temperatures.

2. BACKGROUND

A building's energy demand is characterized by a variable (heating and/or cooling) load profile. Subsequently, the bore field is also subjected to a variable load profile (heat extraction and/or injection). Commercial design software programs widely in use, such as Earth Energy Design (EED) (Hellström & Sanner, 1994) and Ground Loop Heat Exchanger Professional (GLHEPRO) (Marshall & Spitler, 1994), are capable of easily predicting the temperature response due to a variable monthly load profile (repeated over the user's simulation time with a period of a year) for hundreds of bore field configurations, which are contained in their libraries. The procedure implemented in these software programs is based on a sequential superposition of the variable loads over the characteristic temperature response of the bore field, the g-function.

The g-function relates the change in temperature over time at the borehole wall (T_b) from its undisturbed value (T_0) when a constant heat load ($q \times H$) is injected into the bore field, where q represents the average heat extraction per unit length and H is the total active borehole length. This response is obtained from the assumption that pure heat conduction occurs in a homogenous and isotropic surrounding ground medium with the definition of constant temperature (undisturbed value) at the boundaries of the surrounding ground. The g-function is usually represented over a non-dimensional time, defined as the Fourier number with the active borehole length (H) as the characteristic length. ($Fo_H=t/t_s=\alpha t/H^2$ where α is the thermal diffusivity of the ground and $t_s=H^2/9\alpha$ is the characteristic time). The g-function depends on geometrical aspect ratios of the borehole radius (r_b), the borehole spacing (B) and the inactive length (D) to the active borehole length (H). Hence the g-function is distinctive to the geometrical aspect ratios of the borehole field. The g-function is mathematically defined in equation 1

$$T_b - T_0 = \frac{q}{2\pi k} g\left(\frac{t}{t_s}, \frac{r_b}{H}, \frac{B}{H}, \frac{D}{H}\right) \qquad [1]$$

Due to the linear nature of heat conduction the thermal response of the bore field to a variable load can be easily assessed by applying temporal superposition of variable heat pulses over bore field's g-function as shown in Monzó et al. (2015).

When Eskilson introduced the concept of the g-function in 1987 (Eskilson, 1987), both analytical and numerical methods were proposed for the evaluation. However, he favored the numerical solution based on a finite difference method to be utilized in the superposition borehole model (SBM) computer program. Eskilson's reason to opt for the numerical method might be the definition of the boundary condition at the borehole wall. In Eskilson's analytical solution boreholes were represented by finite lines made of a collection of point sources with constant heat flux and an equal heat flow distribution among the boreholes. Eskilson's numerical method allowed the definition of a total heat flow in the bore field and a uniform temperature boundary at all the borehole walls.

For the sake of flexibility, especially in design and optimization targets, exhaustive research activity has been dedicated to the g-function's analytical solutions. The efforts have been focused on finding accurate and fast computational methods for g-functions generation. As a first step to make the analytical solution practical for engineering purposes, simpler expressions of the FLS solution to calculate the mean borehole wall temperature was investigated by Eskilson (1987), Zeng et al. (2002) and more recently by Lamarche and Beauchamp (2007),

Claesson and Javed (2011). The simplifications proposed by (Lamarche and Beauchamp (2007), Claesson and Javed (2011)) were both rapidly solving the FLS expression, which are currently employed in more sophisticated solutions (Cimmino 2014 and 2015 and Lazzarotto 2016). However, the g-functions obtained from pure FLS approaches overestimated the g-function compared to Eskilson's numerical solution. These deviations increase with the number of boreholes and time, (Fossa, 2011), which is attributed to the boundary condition defined at the borehole wall (Monzó et al. 2014). Thus the research community has also strived towards a better representation of the boundary condition at the borehole wall by using a semi-analytical solution based on the FLS solution that divides the borehole into a number of segments in which a different heat flux is applied to each segment. A uniform temperature boundary condition can be represented to a reasonable degree of accuracy using this approach (Cimmino and Bernier 2014, Cimmino 2015). This method has also been used by Lazzarotto (2016) for inclined boreholes. Recently Cimmino (2015) has introduced the inlet fluid temperature as the input to impose the boundary condition at the borehole wall.

Although the long computing time of numerical methods for g-function generation does not make them attractive for engineering purposes, numerical modelling can provide detailed description of the thermal process of bore fields and useful information for research purposes (Monzó et al 2015). Zanchini, et al., (2012) developed a 2D-axisymmetric model with a constant heat flux boundary condition at the borehole wall. Recently, Priarone and Fossa (2016) have also developed a 2D-axisymmetric model in COMSOL Multiphysics®, in which temperature response factors for the single borehole are generated with an adiabatic condition at the top surface and different boundary conditions at the borehole wall: Constant heat flux, constant temperature and uniform temperature boundary using the concept of the highly conductive material embedded in the borehole. Priarone & Fossa,(2016) also presented the g-function of 64 regular patterns in which temporal and spatial superposition of their numerical solution is applied. A complete analysis of the solution for multiple boreholes will be described in a future publication.

3. BAIONA'S GCHP INSTALLATION

3.1. Description of Baiona's GCHP system

The facility under study is an elementary school located in Baiona, Spain, which consists of one building with 800 m^2 of radiant heated floor. This GCHP installation belongs to a demonstration project in the region of Galicia (Iglesias, et al., 2012). The usual occupation of the school is 85 children and 10 workers. The school is open only during weekdays but the GCHP system operates continuously during the whole week. The thermal demands to satisfy are space heating (SPH) (63%) and domestic hot water (DHW) (37%). Until the end of 2009 the school met their heating needs through a 90 kW conventional fuel oil boiler. In January 2010, the boiler was replaced by GCHP system with a heat pump (IDM TERRA 45 S) with nominal capacity of a 52 kW and with R407C as refrigerant. In the building the heat pump is connected to the radiant floor heating system, for SPH and a thermal buffer tank of 1500 liters, which also serves as an instantaneous DHW supply. A schematic of the system is shown in Figure 1.

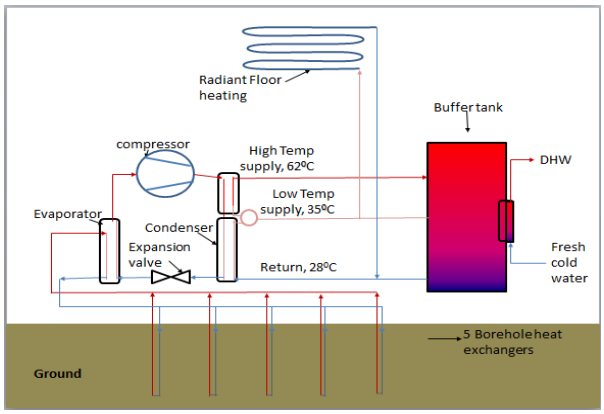

Figure 1: Schematic of the installation at Baiona

The outdoor circuit consists of 5 GHEs connected in parallel, each with a total borehole length of 120 m and with an inactive upper depth of 2 m. The borehole diameter is 140 mm with a double-U PEHD SDR 11 32×2.9 mm geothermal probe. The arrangement of the bore field is shown in Figure 2 and its geometrical aspects ratios are listed in Table 1.

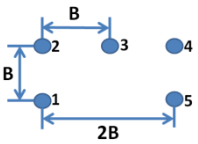

Figure 2: Bore field configuration

During the design phase of the bore field, a thermal response test (TRT) was performed on the bore field to determine the properties of the ground. The results of the TRT are summarized in Table 2.

Table 1: Geometrical aspect ratios of the bore field.

Geometrical aspect ratio	Value
r_b/H	0.0006
B/H	0.0678
D/H	0.0169

Table 2: Ground thermal properties and GHE thermal resistance

Property	Value
Undisturbed ground temperature (T_0)	16.5 ^{0}C
Ground thermal conductivity (k)	2.94 W/(m×K)
Volumetric heat capacity (C)	2.4 MJ/(m^3 ×K)
GHE thermal resistance (Rb)	0.087 (m×K)/W

3.2. Operating and Monitoring Baiona's GSHP system

Some test extraction routines were performed in January 2010, which were not monitored. The normal operation of the installation started in February 2010 and has continued up to now, but the monitoring system has not been functional since January 2014. The present analysis will focus only on the period when the data was collected, i.e., February 2010 to December 2013. The average daily load for the whole monitored period was 124 kWh and the total heat extracted in 2013, which has been considered as a representative year in the present paper, was 47.7MWh.

The monitoring system recorded the power consumed by the compressor and the power consumed by the auxiliary circulation pump of the GHE circuit. The electrical energy meters have an uncertainty of ±5%. Energy flow meters, which are located at the GHE, SPH and DHW circuits, measured the flow rate, and inlet and outlet temperatures. Temperature sensors have an uncertainty of ±0.15, while thermal energy has an uncertainty of ± (0.15 + 2/ΔT) %. The data was logged at 10 minutes intervals. Unfortunately, the data was not logged properly for some periods because of faults in the monitoring system, as listed in Table 3.

Table 3: Periods with lack of measured data and adjustment applied for simulation purposes

Period	Fault	Adjustment
01/02/2010-18/02/2010	Energy reading missing	Energy calculated from power reading
14/10/2010-25/10/2010	No data logged	Daily energy calculated from cumulative energy
29/10/2010-01/11/2010	No data logged	Daily energy calculated from cumulative energy
29/03/2011-10/04/2011	No data logged	Daily energy calculated from cumulative energy
02/01/2012-06/03/2012	No data logged	Daily energy calculated from cumulative energy
21/12/2012-31/12/2012	No data logged	Daily energy calculated from cumulative energy

For simulation purposes, some adjustments have been performed to overcome the periods with loss of measured energy extraction flow. During the period when the energy readings were missing, energy was calculated by integrating the power readings over time. In the other periods where the data was not logged the energy meter was working. The cumulative energy measurements at the beginning and end of the fault period allowed the calculation of the total energy exchanged during these periods. Then, the heat load extracted from the ground was assumed to be distributed evenly over the days of the fault period.

3.3. Energy efficiency of Baiona's GCHP system

The energy efficiency of Baiona's GCHP installation is assessed by defining two system boundaries. The first system boundary accounts only for the heat pump. The energy performance factor of this system boundary (PF_1) evaluates the efficiency of the heat pump refrigeration cycle, which relates the heat rejected (useful heat) into the building, i.e. the sum of heating energy ($Q_{SPH+DHW}$) to provide SPH and DHW, to the electric energy supplied to the compressor (E_{Comp}). The second system boundary comprises the heat pump and the auxiliary circulation pump of the GHE circuit. The energy performance of the second system boundary is evaluated as the ratio of the useful heat ($Q_{SPH+DHW}$) to the electrical energy consumed by the auxiliary circulation pump of the outdoor circuit ($E_{AuxPump}$) and the compressor (E_{Comp}). The performance factors (PF_1 and PF_2) are evaluated for a daily period of time (DPF_1 and DPF_2).

$$DPF_1 = \frac{Q_{SPH+DHW}}{E_{Comp}} \qquad DPF_2 = \frac{Q_{SPH+DHW}}{E_{Comp}+E_{AuxPump}} \quad [2]$$

The DPF_1 and DPF_2 are calculated from Feb 2010 till 18th October 2013. After 18th October 2013 DHW energy measurements were not registered because of a fault in the monitoring system. Figure 3 shows DPF_1 and DPF_2, daily heating energy ($Q_{SPH+DHW}$) as function of the daily entering temperature fluid (ETF) to the heat pump (i.e., outlet fluid temperature of the GHE).

For the overall operation time, the DPF_1 mean value is 4.17 and its standard deviation 0.575 hence DPF_1 of less than 3 and greater than 5.3 are considered not to be representative. As observed in Figure 3, EFT increases as the heating energy decreases. According to the DPF_1 values, we can observe two different performance periods. The 'first performance period' is observed when EFT varies between 7.4^{0}C and approximately 13^{0}C and the SPH demand is larger than DHW demand. In the 'first performance period' the DPF_1 increases as EFT increases, as a decrease of the temperature difference between the source and the sink; which results in a higher cycle efficiency (less compressor work). The 'second performance period' is characterized by unpredictable and dispersed DPF_1 values. In the 'second performance period' the EFT is higher than 13^{0}C and the energy demand due to DHW usually dominates the total heating requirement. In the 'second performance period' the low

values of DPF_1 are related to days with very low energy demand in comparison to the electricity consumed by the compressor. Whereas, high values of DPF_1 (>4.17+2×0.575) result from an increase of the heating energy demand and of the source temperature which indicates that the heating energy is satisfied with a low electricity consumption of the compressor.

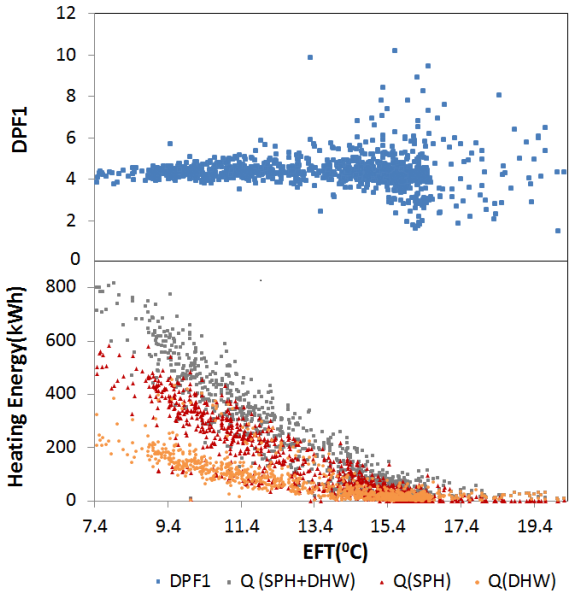

Figure 3: DPF_1 and DPF_2, Heating energy vs ETF

However, at this second performance period, some extremely high DPF_1 values (<8.2) are also observed which is related to intermittent operation of the heat pump for short periods (less than one hour per day) at high temperatures. Hence there is a high probability that the recorded measurement (instantaneous measurement every 10 minutes) is not of a steady state. The non-steady state readings can be identified by checking if the fluid temperature difference between the inlet and outlet of the heat exchanger is significant to represent the operation of the system. When a data filter with a threshold temperature difference of 3 K is applied many non-representative points can be removed. The energy performance of the system based on DPF_2 presents a similar behavior as DPF_1. DPF_2 values are approximately 4% less than DPF_1 values.

4. NUMERICAL MODEL

The thermal response of the bore field is modelled in COMSOL Multiphysics®, a numerical software based on the finite element method (FEM). The model employed in the current study is an improved version of the model presented in (Monzó, et al., 2015).

4.1. Improvements on the HCM model

In the HCM model (Monzó, et al., 2015) a fictitious highly conductive material embedded in the boreholes is used to model the boreholes by cylindrical heat source with an isothermal, i.e. uniform temperature, boundary condition. The thermal connection of the boreholes (connected in parallel) is represented by physically connecting the boreholes (top active surface) through a bar of the same highly conductive material, above the top ground surface. The inactive upper part of the boreholes is handled by auxiliary cone elements that connect the top surface of the active borehole with the bar, on which the total heat flow of the bore field is imposed. The model described in (Monzó, et al., 2015) presented high values of heat flux rate at the top and at the bottom of the borehole, as reported. The intended boundary condition is to have the circulating fluid at a uniform temperature. With the higher heat flux at the ends of the borehole, the temperature drop over the borehole resistance becomes higher and distorts the concept of an isothermal borehole wall. Hence the following modifications are introduced to the HCM model (Monzó, et al., 2015).

1. A thin thermally resistive layer (TRL) is introduced between the HCM and the borehole wall.

The thermal resistance between the fluid and the borehole wall, known as borehole thermal resistance, is represented by introducing a TRL at the borehole wall. Considering the example of Baiona's GCHP installation, a borehole thermal resistance of 0.087 (m×K)/W is represented by a 5 mm thick (arbitrary choice) layer, which surrounds the borehole, at a radius of r_b (0.07 m), and its thermal conductivity corresponds to 0.130 W/(m×K), as obtained from equation 2.

$$R_b = \frac{\delta_{layer}}{2 \cdot \pi \cdot r_b \cdot \lambda_{layer}} \qquad [3]$$

2. A hemi-spherical geometrical element is added at the bottom part of the borehole.

Since sharp edges result in a high heat flux at the corners, the bottom of the borehole is drawn as a hemi-spherical element, Figure 4. The volume of the hemispherical element is $7.18 \cdot 10^{-4}$ m^3.

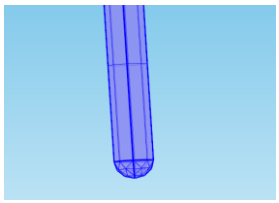

Figure 4: Hemi-spherical bottom element of the borehole in 3D space dimension.

Calculations were performed both by including and excluding the hemi-spherical region in the active length.

The difference in the g-function between the models for short periods (ln(9FoH)=-4.5) was 0.56% and the asymptotic value of g-function (ln(9FoH)=1.5) differed by 0.79%. The difference between the models is negligible as the length of the hemisphere is much smaller than the length of the borehole (0.07m<<118m), Hence the hemi-spherical element at the bottom of the borehole is not taken into account as part of the total active borehole length in the following analysis.

The numerical model that contains the improvements applied to the HCM model is named as 'enhanced HCM model' and labelled as 'EHCM model' in the following sections.

4.2. Modelling Baiona's bore field with the 'enhanced HCM model' (EHCM model)

Baiona's bore field is modelled using the 'EHCM model'. The surrounding ground is represented by a cylinder of radius 150 m and depth 240 m. Taking advantage of the symmetry of the Baiona's bore field pattern, only half of the bore field, with 2.5 boreholes, is modelled, with an adiabatic wall in the plane of symmetry. The bore field geometry was built according to the aspect ratios presented in Table 1. The thermal properties of the ground are defined according to the values listed in Table 2. The initial temperature condition is set equal to the undisturbed measured value at Baiona's GCHP site, as shown in Table 2. An undisturbed temperature condition is defined at the outer boundary of the surrounding ground.

The mesh consists of 186839 elements, which comprises radial elements in the region next to the borehole and tetrahedral elements far from the borehole. The simulations were performed on a computer with an Intel Core i7 2.8GHz processor and 8GB RAM. The computing time for the generation of a g-function for a 200 years period is about 5 hours. The prediction of daily fluid temperature over 4 years of operation requires 5.5 hours.

4.3. Validation of the 'enhanced HCM model': g-function generation

To validate the 'enhanced HCM model', the g-function is generated according to Baiona's bore field and compared with its reference solution obtained from pre-processor (Cimmino & Bernier, 2013). The g-function generation was performed by providing a total constant heat flow in the bore field.

It should be noted that, in the 'enhanced HCM model', the use of TRL results in the temperature in the HCM to be equal to the fluid temperature and the temperature outside the thermal resistive layer to be equal to borehole wall temperature. To avoid the transition region, a distance of $1.01\times r_b$ is chosen for evaluation of the borehole wall temperature. This distance is just enough to avoid the transition region (Puttige, 2016)

Figure 5 shows the g-function corresponding to Baiona's bore field geometry obtained from the previous 'HCM model' with a uniform temperature (UT) boundary condition at the borehole wall (BHW), the 'EHCM' with a uniform fluid temperature (UFT) boundary condition, and a FEM model for constant heat flux (CQ) boundary condition at the borehole wall, which are labelled as 'FEM-HCM UT-BHW', 'FEM-EHCM UFT' and 'FEM CQ', respectively. Their reference solutions obtained from analytical approaches are also shown in Figure 5. 'FLS UT' is the reference g-function obtained from the analytical solution with uniform temperature condition at the borehole wall (Cimmino and Bernier 2013), while 'FLS CQ' represents the g-function obtained for the analytical solution with constant heat flux condition at the borehole wall (Lamarche and Beauchamp 2007).

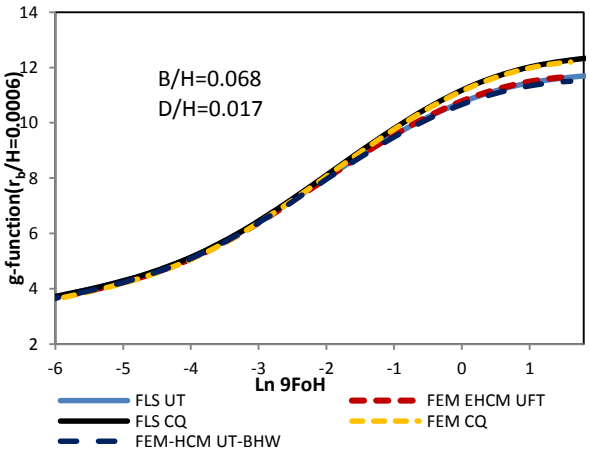

Figure 5: Comparison of g-functions from different models

At short times (ln(9FoH)=-4.5≈162 days), the difference between the 'FEM-EHCM UFT' and the 'FLS UT' is 0.07 units, while the difference between 'FEM CQ' and 'FLS CQ' is 0.1 units. The asymptotic values ($\ln(9Fo_H)$=1.5≈179.5 years) of 'FEM-EHCM UFT' and 'FLS UT' differ by 0.03 units, while 'FEM CQ' and 'FLS CQ' differ by 0.05 units. At short times (ln(9FoH) =-4.5≈162 days) the g-function of 'FEM-EHCM UFT' is 0.01 units higher than 'FEM-HCM UT-BHW', which will result in a negligible temperature difference for a load of 20W/m . However, 'FEM-EHCM UT' is 0.17 units higher than 'FEM-HCM UT-BHW' when ln(9FoH)=1.5 ≈179.5 years, which results in a temperature difference of 0.18 K for a constant heat flux of 20W/m. The 'FEM-EHCM UFT' has a closer agreement with 'FLS UT' compared to the 'FEM- HCM

UT-BHW'. For ln(9FoH)=1.5, the g-function from 'FEM- EHCM UFT' is 0.03 units higher than the value from 'FLS UT' while the 'FEM-HCM UT-BHW' is 0.14 units lower than the 'FLS UT'.

Figure 6 shows the temperature and heat flux profiles at a radius of $1.01r_b$ from the center of borehole number 3 in Figure 2. The heat flux profiles are represented by straight lines and dashed lines are used to illustrate the temperature profiles. In the 'enhanced HCM' model, the heat flux at the bottom and top edges of the borehole have decreased significantly in comparison to the results from the HCM model. In the 'enhanced HCM' the temperature profiles at the borehole wall is not uniform along the borehole length, a gradient of temperature at the edges of the borehole is observed in relation to a higher dissipation of heat at these parts and the borehole thermal resistance.

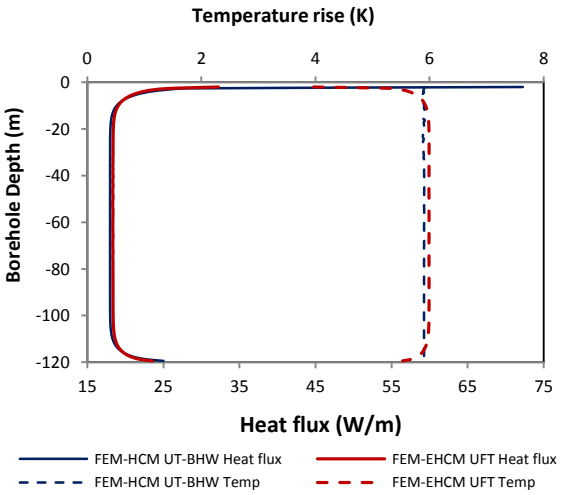

Figure 6: Heat flux and temperature profiles at the boreholes of HCM and EHCM models after 1 year of total constant heat injection.

The difference between the g-function generation using uniform fluid temperature and uniform borehole wall temperature is not significant. However, the definition of a uniform fluid temperature boundary condition, the introduction of the borehole thermal resistance and the hemi-spherical element at the bottom part of the borehole results in a realistic representation of the heat flux and temperature profiles at the borehole wall.

5. FLUID TEMPERATURE PREDICTION AND COMPARISON WITH MEASURED DATA

The measured fluid temperatures are results from daily average of inlet and outlet temperature measurements. Daily average values are results from measurements of 10-minutes intervals, however, the 10 minutes-measurements does not always represent the fluid temperature of the bore field. The heat pump switches off when there is no heating demand. Data points in which volume flow rate in the bore field circuit was equal to zero (heat pump is off) are filtered out.

The 'enhanced HCM' model, the HCM model and a FEM with a constant heat flux boundary condition are used in this paper to predict borehole wall temperatures (T_b). Hence fluid temperatures (T_f) are calculated from T_b, using equation 3.

$$T_f=T_b+q\times R_b \qquad [3]$$

5.1. Prediction of daily fluid temperature and comparison with measured data.

After the 'enhanced HCM model' has been validated for the generation of the g-function, it is employed to simulate daily fluid temperatures. Daily loads from the monitored period at Baiona's GCHP installation, i.e. 3 years and 11 months, were used for the simulation. **Error! Reference source not found.** shows the prediction of the daily fluid temperature obtained from the 'enhanced HCM model' with uniform fluid temperature, HCM model with uniform temperature at the borehole wall, and a FEM with constant heat flux boundary condition at the borehole wall are also illustrated in Figure 7 and labeled as 'Simulated Daily Temp FEM-EHCM UFT', 'Simulated Daily Temp FEM-HCM UT-BHW' 'Simulated Daily Temp FEM QC' respectively. The measured daily fluid temperatures is labeled as 'Measured Daily Temp' and the load profile refer to the secondary y-axis tagged as 'Daily Average Heat Flow' are also shown in Figure 7.

The mean bias error (MBE) of 'Simulated Daily Temp FEM-EHCM UFT' in comparison with 'Measured Daily Temp' is 1.39 K, the mean of absolute error (MAE) is 1.58 K and the root mean square error (RMSE) is 1.77 K. As observed in Figure 7, the error of 'Simulated Daily Temp FEM-EHCM UFT' (against 'Measured Daily Temp') is higher for the first two years than in the last monitored year. In the first two years the error is characterized by a MBE of 1.61 K and the RMSE is 2.11 K, whereas the MBE and RMSE for the last year are 0.94 K and 1.25 K, respectively. This is probably due to the unrecorded early load of the ground, which was not considered in the simulation.

The maximum deviation in 2010 occurs in the first few days, this is expected as the influence of tests performed in January 2010 will be the most during the first few days, as shown in Table 4. The total MBE and RMSE are reduced by 17% and 13% respectively when the influence of the operation in January is accounted for, according to the procedure established in section 5.2. With the exception of the error observed during the first

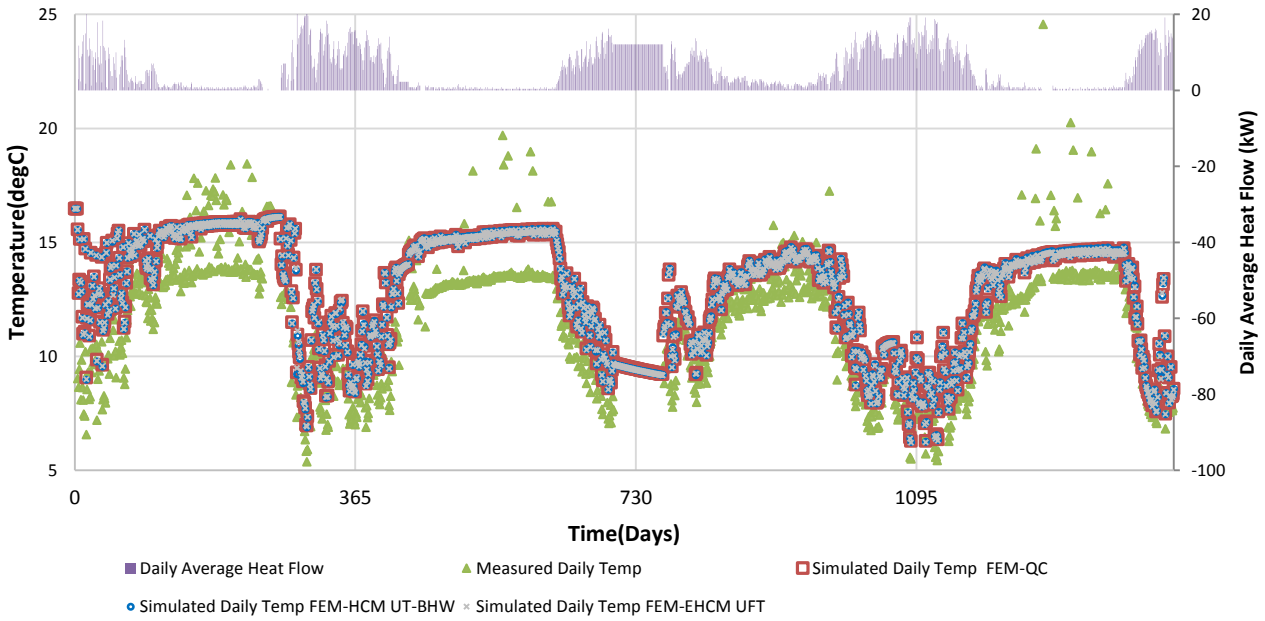

Figure 7: Daily fluid temperature predictions using FEM models and comparison with measured data

year, in the remaining years the maximum error occurs in summer where some odd high temperatures are observed. The raw measured data is obtained from particular points taken every 10 minutes.

The response time of temperature sensors are typically much higher than response time of flow measurement devises. A measurement recorded in the time frame between the response time of the flow measurement and the temperature measurements would explain the odd high temperatures. Such readings are more likely to occur in summer because the flow in the boreholes occurs for short durations in summer as the load is lower. Hence these points do not represent the fluid temperature in the borehole.

The MBE of daily fluid temperature predictions of 'FEM HCM UT-BHW' is 1.41 K, while the RMSE is 1.79 K. Similar to the 'FEM EHCM UFT' model the deviation in the first two years (MBE 1.68 K and RMSE 2.02 K) is higher than the last year (MBE 0.99 K and RMSE 1.29 K). The predictions of 'FEM EHCM UFT' are closer to the measured data than 'FEM HCM UT-BHW' for all years. The overall MBE is 0.02 K lower for 'FEM EHCM UFT' model, and in the last year the difference is 0.04 K. The order of the difference between the models can be estimated using the difference in g-function, for example the difference in g-function for 4 years (ln(9FoH)=-2.3) is 0.03 for a constant heat load of 8.75 W/m (which is the average load of the installation) this results in a temperature difference of 0.012 K. The magnitude of reduction in error between the models is too small to conclusively state that the fluid temperature predictions are better in 'FEM EHCM UFT',

As mentioned earlier, temporal superposition of variable loads over the g-function is a common procedure to evaluate fluid temperatures of GSHP installations. In our studies we have also employed this procedure and compared it with its corresponding data resulting from the 'enhanced HCM model' and variable load input. The difference between the fluid temperature predictions from superposition of the reference g-function (SP-FLS UT) and 'FEM EHCM UFT' were negligible, The MBE of 'SP FLS UT' is 1.40 K and MAE is 1.59 K, this differs from 'FEM EHCM UFT' by 0.008 K and 0.005 K respectively. The close agreement of the models further verifies the correctness of the EHCM model.

5.2 Effect of test operation performed during January 2010, before normal operation of Baiona's GCHP installation.

Several test-operations were performed at the Baiona's GCHP installation during January 2010. The influence of these tests on the prediction of the simulation fluid temperatures is quantified by imposing an equivalent load for this test period. A zero load is applied for the rest of the simulated period. Since it is assumed that before January 2010 the ground temperature remains at its undisturbed value and the temperatures were registered since the beginning of the normal of operation of the GCHP, the equivalent load is calculated by analyzing the change of the borehole wall temperature to its undisturbed estimation and the g-function value corresponding to the test period. Hence, the first

monitored day, after test operation, was 4th February 2010, i.e., 34 days after 1st January 2010 (initial time of test operation), which corresponds to a ln(9FoH) =-6.1 and a g-value = 3.6. The average daily fluid temperature recorded on 4th February 2010 is 9.05^{0}C; which represents a change of temperature ($T_b - T_0$) of 7.4^{0}C, from equation (1) is obtained that a constant heat flux extraction of 37.84 W/m represents the test operation carried out during January 2010.

Table 4: Effect of Jan 2010 pulse

Time period	effect of Jan 2010 pulse on the ground temperature (K)
30 days	-2.9
next 3 months	-0.6
rest of 2010	-0.3
2011	-0.2
2012	-0.1
2013	-0.1

The analysis indicates that the operation in January 2010 significantly affects the ability of the model to predict the fluid temperature for the first few days but the effect decreases exponentially. The temperature effect is around 0.24 K after a year of operation. Table 4 summarizes the effect of operations in January 2010 for different periods. The high deviation of the model compared to the measured data for the first 4 months of operation can be explained as an effect of ignoring the activities in January 2010.

5.3. Monthly analysis for 50 years

As non-observable difference were detected between 'Simulated Daily Temp FEM-EHCM UFT' and 'Simulated Daily Temp FEM CQ' during the first four years of operation.

The g-function comparison indicates that differences may be expected for values of ln (9FoH) higher than -1.7 (≈7.5 years according to Baiona's GCHP installation). A simulation of monthly mean fluid temperature is performed for a reasonable life time of the GCHP installation (50 years) by repeating the yearly load of 2013 throughout the extended period. The results of this simulation are shown in Figure 8, in which 'Simulated Monthly Temp FEM-EHCM UFT' represents the fluid temperature prediction generated from the 'enhanced HCM model' with a uniform fluid temperature boundary condition and 'Simulated Monthly Temp FEM CQ' are monthly fluid temperature predictions obtained from a FEM with a constant heat flux boundary condition at the borehole wall. Monthly predictions are also generated from a commercial software (Hellström & Sanner, 1994), labeled as 'Simulated Monthly Temp Commercial Software'. The secondary y-axis shows the deviation between 'Simulated Monthly Temp FEM-EHCM UFT' and 'Simulated Monthly Temp FEM CQ'. As expected, their differences are more prominent for longer time durations. For example, in the 50th year (ln(9FoH) ≈0.2), the MBE is 0.42 K (0.43 K RMSE). It is observed that the results from 'Simulated Monthly Temp FEM CQ' and 'Simulated Monthly Temp Commercial Software' presents an unexpectedly closer behavior compared to the prediction from 'Simulated Monthly Temp FEM-EHCM UFT', with MBE 0.026K and RMES deviation of 0.12K. Another observation is that the average fluid temperature of the 50th year decreases by about 2.9 K in comparison with the value in the 1st year. This means that if the heat pump operates under similar conditions of the current load (2013), without any heat injection operation, the heat pump will present around 9% penalty on its performance.

6. CONCLUSIONS

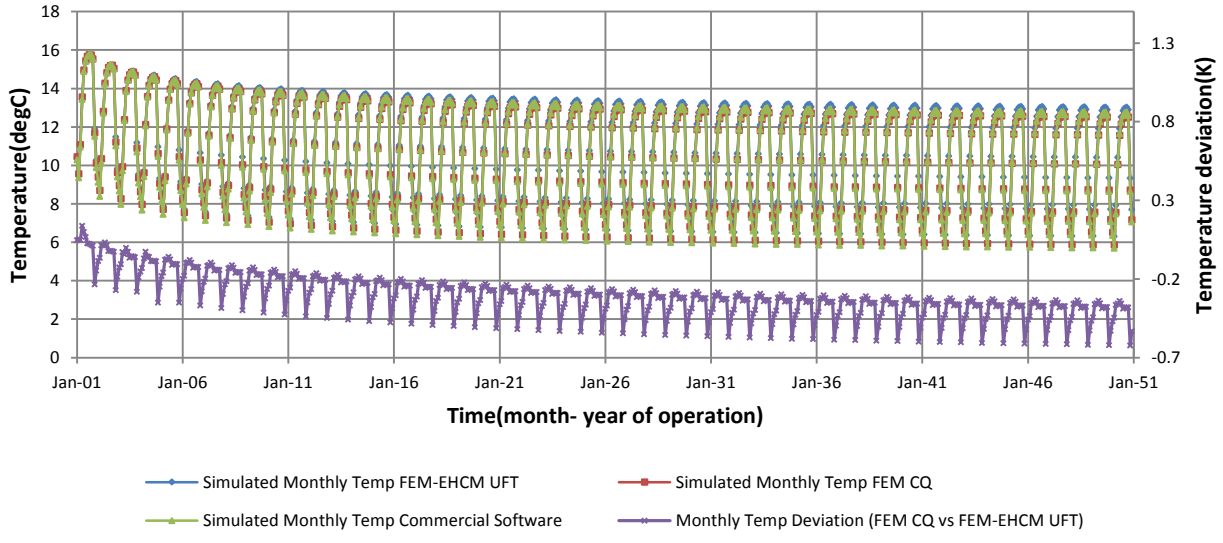

Two simultaneous boundary conditions are usually applied to mathematical approaches of ground heat exchangers connected in parallel: a total bore field heat flow (equal to the energy required by the heat pump) and a uniform temperature boundary condition at all the borehole walls. However, the fact that there is a borehole thermal resistance between the fluid and the borehole wall and that the heat flux increases at the borehole ends result in temperature changes between borehole wall and the fluid. Thus the borehole wall temperature deviates from the uniform assumption and will cause an error in the simulations. This paper describes improvements applied to a previous numerical approach, in which a uniform temperature boundary condition is defined in all the boreholes. The improvements are applied to define a uniform fluid temperature boundary condition instead of a uniform temperature at all the borehole walls. The improved model is validated for the g-function generation. No relevant deviations are observed in the g-function generated from a uniform fluid temperature boundary condition in comparison with reference solutions obtained from a uniform temperature boundary condition at the borehole wall. However, the improvements applied to the previous numerical model results in a realistic representation of the heat flux and temperature profiles at the borehole wall. The improved model is also utilized to illustrate daily fluid temperature predictions for variable measured daily loads of a monitored GCHP installation (52 kW) in Baiona (Galicia, Spain). The daily fluid temperature predictions deviate from the measured data by 0.94 K (MBE) (RMSE 1.25 K) for the last year of simulation. Although the predictions obtained from the improved model are closer to measured values than the predictions from the previous model, the reduction in deviation against measured data is too small (0.02 K in average) to conclusively state that the fluid temperature predictions are better represented by the improved model.

7. REFERENCES

Arrizabalaga, I. et al., 2015. *Country Update for the Spanish Geothermal Sector.* Melbourne, s.n., pp. 1-9.

Cimmino, M. & Bernier, M., 2013. *Preprocessor for the generation of g-function used in the simulation of geothermal systems.* Chambery, France, Building simulation 2013.

Cimmino, M. & Bernier, M., 2014. A semi-analytical method to generate g-functions for geothermal bore fields. *International Journal of Heat and Mass Transfer,* Volume 70, pp. 641-650.

Cimmino, M. & Bernier, M., 2015. Experimental determination of the g-functions of a small-scale geothermal borehole. *Geothermics,* Volume 56, pp. 60-71.

Cullin, J. R. & Spitler, J. D., 2011. A computationally efficient hybrid time step methodology for simulation of ground heat exchangers. *Geothermics,* Volume 40, pp. 144-156.

Eskilson, P., 1987. *Thermal Analysis of Heat Extraction Boreholes,* Lund: University of Lund, Sweden.

Fossa, M., 2011. A fast method for evaluating the performance of complex arrangements of borehole heat exchangers. *Science and Technology for the Built Environment,* 17(6), pp. 948-958.

Gehlin, S. et al., 2015. *Country Update for Sweden.* Melbourne, s.n.

Hellström, G. & Sanner, B., 1994. *Earth energy designer: software for dimensioning of deep boreholes for heat extraction,* Lund: Department of Mathematical Physics, Lund University.

Iglesias, M., Rodríguez, J. & Franco, D., 2012. *Monitoring of building heating and cooling systems based on geothermal heat pump in Galicia (Spain).* Jülich, EDP Sciences.

Ingersoll, L. & Plass, H., 1948. Theory of the ground pipe heat source for the heat pump. *ASHRAE Transactions,* Volume 54, pp. 339-345.

Lamarche, L. & Beauchamp, B., 2007. A new contribution to the finite line-source model for geothermal boreholes. *Energy and Buildings,* Volume 39, pp. 188-198.

Lazzarotto, A., 2016. A methodology for the calculation of response functions for geothermal fields with arbitrarily oriented boreholes Part 1. *Renewable Energy,* Volume 86, pp. 1380-1393.

Lazzarotto, A. & Bjork, F., 2016. A methodology for the calculation of response functions for geothermal fields with arbitrarily oriented boreholes e Part 2. *Renewable Energy,* Volume 86, pp. 1353-1361.

Marshall, C. & Spitler, J., 1994. *GLHEPRO – The Professional Ground Loop HeatExchanger Design Software, Users' Guide* School of Mechanical and Aerospace Engineering. Oklahoma State University.

Monzó, P. et al., 2015. A novel numerical approach for imposing a temperature boundarycondition at the borehole wall in borehole fields. *Geothermics,* Volume 56, pp. 35-44.

Priarone, A. & Fossa, M., 2016. Temperature response factors at different boundary conditions for modelling the single borehole heat exchanger. *Applied Thermal Engineering,* Volume 103, p. 934–944.

Zanchini, E., Lazzari, S. & Priarone, A., 2012. Long-term performance of large borehole heat exchanger fields with unbalanced seasonal loads and groundwater flow. *Energy,* Volume 38, pp. 66-77.

Zeng, H. Y., Diao, N. R. & Fang, Z. H., 2002. A Finite Line-Source Model for Boreholes in Geothermal Heat Exchangers. *Heat Transfer—Asian Research,* 31(7), pp. 558-567.